This MICCAI paper is the Open Access version, provided by the MICCAI Society. It is identical to the accepted version, except for the format and this watermark; the final published version is available on SpringerLink.

Gyri vs. Sulci: Core-Periphery Organization in Functional Brain Networks

Xiaowei Yu[1], Lu Zhang[1], Chao Cao[1], Tong Chen[1], Yanjun Lyu[1], Jing Zhang[1], Tianming Liu[2], and Dajiang Zhu[1]

[1] The University of Texas at Arlington, Arlington TX 76019, USA
{xxy1302,lu.zhang2,cxc0366,txc5603,jxz7537,yxl9168}@mavs.uta.edu, dajiang.zhu@uta.edu
[2] University of Georgia, Athens GA 30602, USA
tliu@uga.edu

Abstract. The human cerebral cortex is highly convoluted into convex gyri and concave sulci. It has been demonstrated that gyri and sulci are significantly different in their anatomy, connectivity, and function: besides exhibiting opposite shape patterns, long-distance axonal fibers connected to gyri are much denser than those connected to sulci, and neural signals on gyri are more complex in low-frequency while sulci are more complex in high-frequency. Although accumulating evidence shows significant differences between gyri and sulci, their primary roles in brain function have not been elucidated yet. To solve this fundamental problem, we design a novel Twin-Transformer framework to unveil the unique functional roles of gyri and sulci and their relationship in the whole brain function. Our Twin-Transformer framework adopts two structure-identical (twin) Transformers to disentangle spatial-temporal patterns of functional brain networks: one focuses on the spatial patterns and the other is on temporal patterns. The spatial transformer takes the spatially divided patches and generates spatial patterns, while the temporal transformer takes the temporally split patches and produces temporal patterns. We validated our Twin-Transformer on the HCP task-fMRI dataset, to elucidate the different roles of gyri and sulci in brain function. Our results suggest that gyri and sulci could work together in a core-periphery network manner, that is, gyri could serve as core networks for information gathering and distributing, while sulci could serve as periphery networks for specific local information processing. These findings have shed new light on our understanding of the brain's basic structural and functional mechanisms.

Keywords: Gyri and Sulci · Core-Periphery · Twin-Transformer.

1 Introduction

Gyri and sulci are the standard morphological and anatomical nomenclature of the cerebral cortex (Figure 1) and are usually defined in anatomical domains [1].

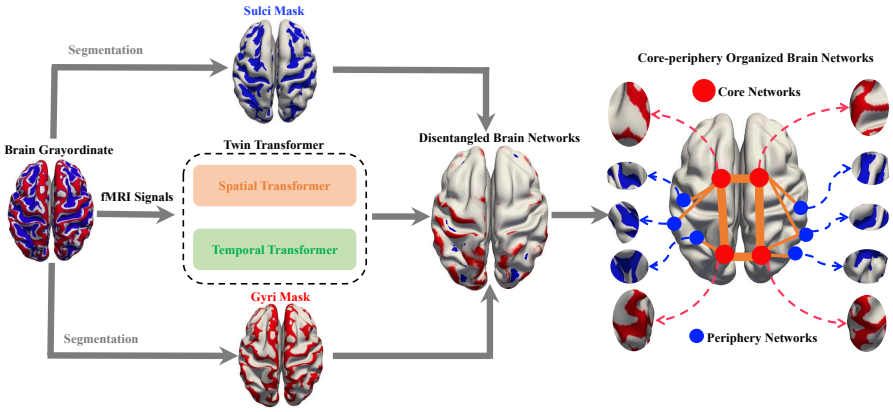

Fig. 1. Core-periphery organized brain networks in gyri and sulci. The fMRI signals extracted from voxels are fed into the Twin-Transformer model. The disentangled brain networks are organized in a core-periphery manner, where gyri serve as the core network, and sulci serve as the periphery network.

Gyri and sulci serve as the basic building blocks to make up complex cortical folding patterns and are fundamental to realizing the brain's basic structural and functional mechanisms. Numerous efforts have been devoted to understanding the function-anatomy patterns of gyri and sulci from various perspectives, including genetics [2], cell biology [3], and neuroimaging [4, 30]. It has been demonstrated consistently that gyri and sulci are significantly different in their anatomy, connectivity, and function. Several studies [6, 19] found that the formation of gyri/sulci may be closely related to the micro-structure of white matter. For example, diffusion tensor imaging (DTI) derived long-distance axonal fibers connected to gyri are significantly denser than those connected to sulci [11]. That is, the long-distance fiber terminations dominantly concentrate on gyri rather than sulci, and interestingly, this phenomenon is evolutionarily preserved across different primate species. Meanwhile, using functional magnetic resonance imaging (fMRI), a few functional measurements that can directly reflect brain functional activities on gyri and sulci have been explored, such as functional BOLD signals [4], correlation-based connectivity/interaction [5, 10, 20], and spatial distribution of functional networks [7, 16]. Despite accumulating functional differences found between gyri and sulci, their basic roles as well as their relationship and interaction in the whole brain function have not been explored or elucidated yet.

To answer this fundamental question in brain science, we proposed a novel Twin-Transformer framework to explore and unveil the unique functional roles of gyri and sulci. Unlike traditional factorization-based approaches that assume linearity and independence, the transformer with self-attention mechanism [14] is an ideal backbone to characterize, represent and reveal the complex and deeply buried patterns in the observed brain functional data. The whole framework is illustrated in Figure 2. Our Twin-Transformer framework adopts two structure-

identical (twin) Transformers to model and disentangle spatial-temporal patterns of gyri and sulci: one focuses on the spatial patterns and the other focuses on temporal patterns. To model the complex 4D (spatial-temporal) fMRI signals, within the framework, we designed a spatial transformer and a temporal transformer to disentangle and extract the patterns in both spatial and temporal domains from the original fMRI signals. After the model is well-trained, the spatial-temporal functional brain networks (FBNs) [15] specific to gyri and sulci can be recovered through gyri and sulci masks. We validated our Twin-Transformer on one of the largest brain imaging datasets (HCP task-fMRI gray-ordinate dataset), for the first time, to elucidate the different roles of gyri and sulci in brain function. Our results suggest that gyri and sulci could work together in a core-periphery network manner, that is, gyri could serve as core networks for information gathering and distributing in a global manner, while sulci could serve as periphery networks for specific local information processing. These findings have shed new light on our fundamental understanding of the brain's structural and functional mechanisms, provide further inspiration for brain-inspired neural network design [12, 13], and aid in the research of brain diseases [21–29]. The contributions of this paper are summarized as follows:

- We proposed a novel Twin-Transformer framework to disentangle the spatial-temporal patterns of the functional brain networks from fMRI datasets.
- We used the proposed method to represent and unveil the fundamental functional roles of the two basic cortical folding patterns: gyri and sulci.
- We found that gyri and sulci may work together in a Core-Periphery network manner: gyri serve as core networks for information gathering and distributing, while the sulci serve as periphery networks for specific local information processing.

2 Methods

2.1 Data Preparation

We use the task fMRI (tfMRI) from the Human Connectome Project (HCP) dataset [17]. The publicly available preprocessed tfMRI data went through the minimal preprocessing pipelines specially designed for the HCP dataset [4]. The preprocessed tfMRI are 4D imaging data, which consists of a time series of 3D images of the brain. For emotion, gambling, language, motor, relational, social, and working memory (WM) task-fMRI, each voxel contains a series of brain signals of time length 176, 254, 316, 284, 232, 274, and 405. We rearrange the signals in each voxel into a 2D matrix. In this way, a 4D tfMRI imaging can be represented by a 2D matrix, where each row stores brain signals at each time step, and each column stores brain signals in a specific voxel (Figure 2-a,b). We normalized the brain signals to zero mean and unit variance [18]. Since each subject of the preprocessed data has 59,412 voxels in standard gray ordinate space, the column dimension of the 2D matrix is 59,412. To facilitate patch partition, we expand the space dimension according to our needs by adding

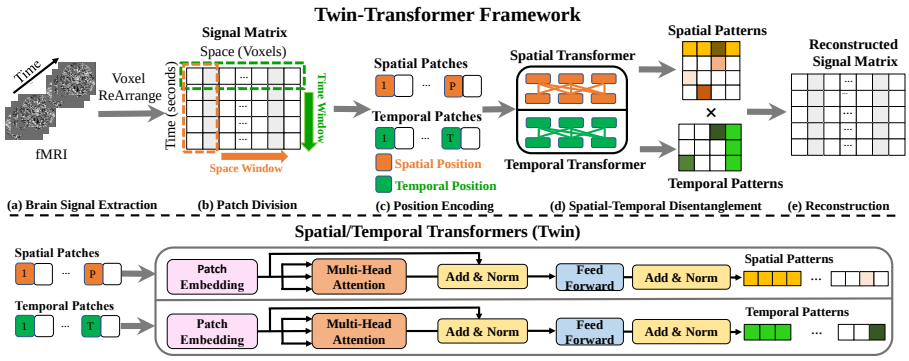

Fig. 2. Illustration of the proposed Twin-Transformer framework. Part (a) extracts the signals and rearranges them into a signal matrix. Part (b) shows the patch division of the signal matrix. Part (c) is the position encoding for the spatial and temporal patches. Part (d) is the Twin-Transformer, which includes spatial and temporal transformers for processing spatial and temporal patches. Part (e) is the reconstruction of the signal matrix from disentangled spatial and temporal patterns. The spatial/temporal transformers under the black dot line show the details of the Twin-Transformer.

zero vectors along the spatial dimension. For example, to disentangle the signal matrices into 50 spatial-temporal brain networks, the space dimension is extended from 59,412 to 59450 to divide the space dimension into 50 patches.

2.2 Twin-Transformer

The architecture of the Twin-Transformer is illustrated in Figure 2. There is a spatial and temporal transformer for disentangling spatial and temporal patterns of the brain networks, as shown in Figure 2-d. The structure of the spatial transformer is identical to the temporal transformer, except they take spatial/temporal divided patches as input. For each input signal matrix, spatial patches are generated by shifting the spatial window along the space dimension, as illustrated by the orange arrow in Figure 2-b, while temporal patches are generated by shifting the temporal window along the time dimension, as shown in the green arrow.

Specifically, within the spatial transformer, the self-attention operation across the spatial patches aims to learn the latent representations of spatial features and takes non-overlapping spatial patches as tokens to build attention across the spatial variant patches and generate spatial patterns. It divides the input signal matrix into P non-overlapping patches by shifting the sliding window (orange dotted box following orange arrow) from left to right along the space dimension. The size of the sliding window can be adjusted according to the size of the input data. Each spatial patch contains partial spatial but complete temporal information on the focal brain region. The P patches correspond to P patterns of brain networks. Patches are used as tokens, and each token is first fed into a linear projection layer to obtain the latent representation $z_i \in \Re^{1\times D_1}$

and then the learnable spatial positional embedding, $E_i^s \in \Re^{1\times D_1}$ is added to the representations of each input token. The spatial transformer encoder can be formulated as:

$$Spa(Z) = MLP(MSA(LN(z_1^s||z_2^s||z_3^s||...||z_P^s))) \tag{1}$$

where MSA() is the multi-head self-attention, MLP() represents multilayer perceptron, and LN() is layernorm. $z_i^s = (z_i + E_i^s)$, $i = 1, 2, ..., P$ and $||$ denotes the stack operation. $Spa(Z) \in P \times N$ is the output of the spatial Transformer, where P represents the number of brain networks, and N is the number of voxels in the brain. $Spa(Z)$ models the activated status of voxels within each brain network.

The temporal transformer is designed to learn the latent representations of temporal patterns of brain networks. Similar to the spatial transformer, by shifting the sliding window (green dotted box following green arrow) from top to bottom along the time dimension, T non-overlapping temporal patches are generated. Each temporal patch contains partial temporal but complete spatial information of all the voxels. Correspondingly, the temporal transformer builds attention across the temporal variant patches and generates temporal features. The sliding window slides each unit of time, so the number of patches equals the length of the signals. After patch embedding and positional embedding, each patch is represented by $z_i^t = (z_i + E_i^t)$, $i = 1, 2, ..., T$. The temporal self-attention module can be formulated as:

$$Tem(Z) = MLP(MSA(LN(z_1^t||z_2^t||z_3^t||...||z_T^t))) \tag{2}$$

The outputs $Tem(Z)$ of the temporal self-attention module have a dimension of $Tem(Z) \in T \times P$, where T represents the time length of the fMRI signals. $Tem(Z)$ represents the temporal patterns of the brain networks. Taking $Spa(Z)$ and $Tem(Z)$ together, we can obtain both the spatial and temporal patterns of the brain networks of each subject.

2.3 Loss Function

There are two terms in the loss function. The first one is the signal matrix reconstruction loss. The whole framework is trained in a self-supervised manner, therefore, the input signal matrix can be reconstructed from the learned spatial and temporal patterns. This is crucial to ensure the learned spatial and temporal features can capture the complete spatial and temporal information of the input data. The reconstruction loss is formulated as:

$$L_{reco} = \sum \|X - Tem(Z) \cdot Spa(Z)\|_{L1} \tag{3}$$

where X is the input signal matrix, and we use the L1-norm to constrain the reconstruction term. In order to make spatial patterns distinct and limit the scale of temporal patterns from being arbitrarily large, we add a normalization on temporal patterns, which is formulated as:

$$L_{tem\_norm} = max(0, \frac{1}{P}(\sum_{i=1}^{P} \|Tem(Z_i[*, i])\|_2) - 1) \tag{4}$$

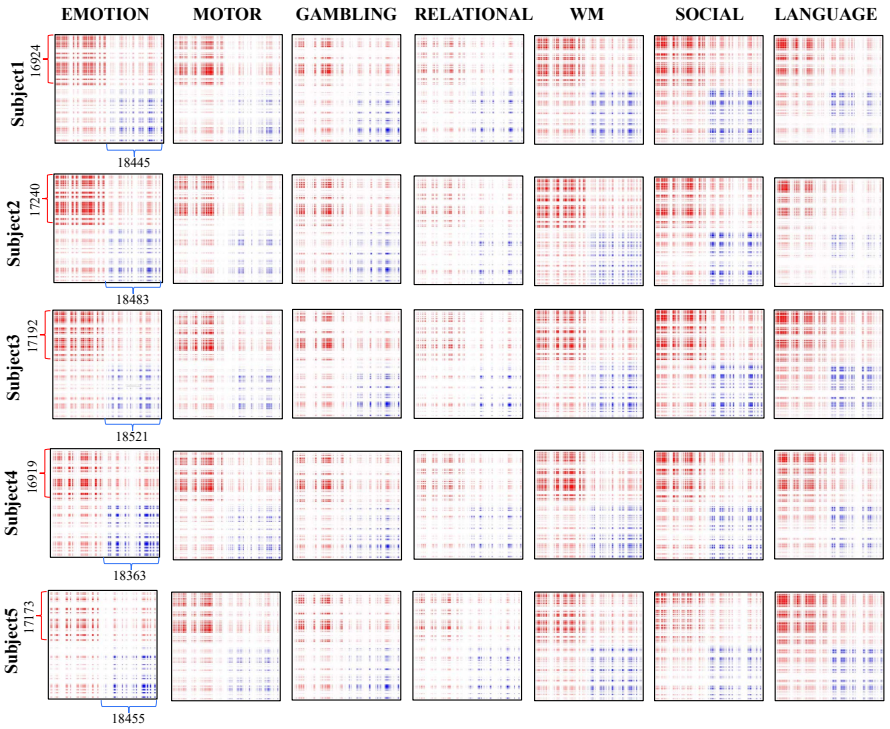

Fig. 3. Relationship matrix of gyri and sulci. Each row represents a subject. Each column represents a task. For each subject, the number of voxels in gyri and sulci are marked in red and blue. The connections between gyri-gyri, gyri-sulci, and sulci-sulci are shown in red, pink, and blue, respectively. These relationship matrices are generated under threshold 0.8.

Combining the two parts, the overall loss can be formulated as:

$$L = L_{reco} + \alpha L_{tem\_norm} \tag{5}$$

where the regularization parameter α controls the influence of temporal normalization on the overall loss function.

3 Results

Using the gray-ordinate fMRI signals of each subject, as input for the Twin-Transformer, the output of the well-train model includes spatial-temporal patterns, where spatial patterns can be interpreted as FBNs, and the corresponding temporal patterns can be treated as the representative signals of each FBN. Though signals on gyri and sulci are different, we set the same threshold. The activated voxels of gyri and sulci in each FBN can be obtained by applying

Table 1. The normalized independent probability of gyri and sulci brain networks under 100 patterns set, and the threshold is 0.8. The format is Mean(Variance).

IP	Emotion	Motor	Gambling	Relational	WM	Social	Language
P_{GG}	0.51(0.03)	0.54(0.03)	0.44(0.05)	0.44(0.03)	0.48(0.03)	0.46(0.03)	0.53(0.03)
P_{GS}	0.30(0.01)	0.30(0.01)	0.32(0.01)	0.32(0.01)	0.31(0.01)	0.32(0.01)	0.30(0.01)
P_{SS}	0.18(0.02)	0.17(0.02)	0.24(0.04)	0.24(0.03)	0.22(0.02)	0.22(0.02)	0.24(0.04)

the gyri and sulci mask to the FBN (Figure 1). We present the core-periphery organization of gyri and sulci, validation, and ablation study in the following subsections.

3.1 Core-Periphery Organization of Gyri and Sulci

We can identify the activated brain voxels in gyri and sulci whose weights are consistently above a pre-defined threshold across all spatial patterns. By connecting all the activated voxels, we can construct a relationship matrix of gyri and sulci and obtain their mapping on the brain surface. We randomly select 5 subjects and present their relationship matrix in Figure 3. Since the number of voxels in gyri and sulci of different subjects are various, the size of the relationship matrices is various. In general, the relation matrix is sparse, which means only a few regions (voxels) are involved in a specific task at the same time. As shown in Figure 3, the activated brain voxels in the gyri-gyri section incline to form larger and connected blocks or clusters, while the activated brain voxels in the sulci-sulci section tend to assemble as smaller and scattered patterns. Besides, compared to relational, other tasks, such as WM, social, language, and emotion involve larger sulcal regions that host more high-level functions.

To examine and prove the concept of the Core-Periphery organization of gyri and sulci, we compute the normalized independent probability (IP) P_{GG}, P_{SS} and P_{GS} for sub-matrices A_{GG}, A_{SS}, and A_{GS} of the relationship matrix, which represents the interactions within gyri vertices (Core Network), sulci vertices (Periphery Network), and between gyri and sulci vertices (between Core and Periphery Networks). Independent probability [8] is defined as the probability that there is an edge between any pairs of nodes in a given matrix, and it is an important measurement to indicate if the matrix or graph is organized as Core-Periphery pattern [9]. The independent probability and normalized independent probability are formulated as:

$$\begin{aligned} I_{GG} = \frac{1_{A_{GG}}}{\|A_{GG}\|_1}, I_{GS} = \frac{1_{A_{GS}}}{\|A_{GS}\|_1}, I_{SS} = \frac{1_{A_{SS}}}{\|A_{SS}\|_1}, \\ P_{GG} = I_{GG}/I, P_{GS} = I_{GS}/I, P_{SS} = I_{SS}/I. \end{aligned} \tag{6}$$

where $I = I_{GG} + I_{GS} + I_{SS}$, $1_{A_{GG}}$ represents the number of 1s in the sub-matrix of gyri-gyri and $\|\bullet\|_1$ is the number of elements in this sub-matrix. The same procedure was applied to sub-matrices of gyri-sulci and sulci-sulci, respectively. We calculate the normalized independent probability, and the averaged results of

Table 2. The normalized independent probability of gyri and sulci brain networks under 100 patterns set, and the threshold is 0.9. The format is Mean(Variance).

IP	Emotion	Motor	Gambling	Relational	WM	Social	Language
P_{GG}	0.59(0.07)	0.57(0.07)	0.53(0.11)	0.49(0.08)	0.52(0.07)	0.55(0.07)	0.65(0.06)
P_{GS}	0.28(0.03)	0.28(0.02)	0.29(0.03)	0.31(0.02)	0.30(0.02)	0.29(0.03)	0.25(0.03)
P_{SS}	0.14(0.04)	0.15(0.04)	0.18(0.08)	0.20(0.06)	0.18(0.05)	0.16(0.05)	0.10(0.03)

Table 3. The normalized independent probability of gyri and sulci brain networks under 100 patterns set, and the threshold is 0.7. The format is Mean(Variance).

IP	Emotion	Motor	Gambling	Relational	WM	Social	Language
P_{GG}	0.43(0.02)	0.42(0.02)	0.44(0.01)	0.45(0.02)	0.41(0.02)	0.42(0.03)	0.41(0.01)
P_{GS}	0.32(0.01)	0.33(0.01)	0.32(0.01)	0.32(0.01)	0.33(0.01)	0.33(0.01)	0.33(0.01)
P_{SS}	0.24(0.01)	0.25(0.02)	0.24(0.01)	0.23(0.01)	0.26(0.01)	0.25(0.02)	0.26(0.01)

group level are shown in Table 1. The results show that $P_{GG} > P_{GS} > P_{SS}$, which confirms that the derived brain networks of gyri and sulci have the core-periphery organization.

3.2 Validation and Ablation Study

We conduct ablation studies to validate the robustness of the proposed Twin-Transformer framework and verify the core-periphery relationship of gyri and sulci under different thresholds. The normalized independent probability of the relationship matrix under thresholds of 0.7 and 0.9 are shown in Tables 2 and 3, respectively. We can observe that the normalized independent probability of the relationship matrix of gyri and sulci under different experimental settings and pre-defined thresholds all satisfy $P_{GG} > P_{GS} > P_{SS}$, which further demonstrates that the gyri-sulci functional brain networks are organized in a core-periphery manner.

4 Conclusion

In this work, we proposed a novel data-driven Twin-Transformer framework and applied it to the HCP gray-ordinate tfMRI dataset to characterize the roles of cortical gyri and sulci on the functional brain networks. With this framework, we can disentangle the spatial and temporal patterns from the brain signals, providing us the possibility to analyze the difference between gyri and sulci. The most important finding in this study is that we identified the core-periphery relationship between gyri and sulci, as well as the corresponding core-periphery brain networks. Our results show that core-periphery networks broadly exist between gyri and sulci across different subjects and tasks. Overall, our proposed Twin-Transformer contributes to a better understanding of the roles of gyri and sulci as core and periphery in brain architecture.

Acknowledgments. This work was supported by National Institutes of Health (R01AG075582 and RF1NS128534).

Disclosure of Interests. The authors have no competing interests to declare that are relevant to the content of this article.

References

1. Jiang, X., Zhang, T., Zhang, S., Kendrick, K.M. and Liu, T.: Fundamental functional differences between gyri and sulci: implications for brain function, cognition, and behavior. Psychoradiology, 1(1), pp.23-41 (2021).
2. Richiardi, J., Altmann, A., Milazzo, A.C., Chang, C., Chakravarty, M.M., Banaschewski, T., Barker, G.J., Bokde, A.L., Bromberg, U., Büchel, C. and Conrod, P.: Correlated gene expression supports synchronous activity in brain networks. Science, 348(6240), pp.1241-1244 (2015).
3. Gertz, C.C. and Kriegstein, A.R.: Neuronal migration dynamics in the developing ferret cortex. Journal of Neuroscience, 35(42), pp.14307-14315(2015).
4. Liu, H., Zhang, S., Jiang, X., Zhang, T., Huang, H., Ge, F., Zhao, L., Li, X., Hu, X., Han, J. and Guo, L.: The cerebral cortex is bisectionally segregated into two fundamentally different functional units of gyri and sulci. Cerebral Cortex, 29(10), pp.4238-4252 (2019).
5. Deng, F., Jiang, X., Zhu, D., Zhang, T., Li, K., Guo, L. and Liu, T.: A functional model of cortical gyri and sulci. Brain structure and function, 219(4), pp.1473-1491 (2014).
6. Hilgetag, C.C. and Barbas, H.: Developmental mechanics of the primate cerebral cortex. Anatomy and embryology, 210(5), pp.411-417 (2005).
7. Lv, J., Jiang, X., Li, X., Zhu, D., Zhang, S., Zhao, S., Chen, H., Zhang, T., Hu, X., Han, J. and Ye, J.: Holistic atlases of functional networks and interactions reveal reciprocal organizational architecture of cortical function. IEEE Transactions on Biomedical Engineering, 62(4), pp.1120-1131 (2014).
8. Cucuringu, M., Rombach, P., Lee, S.H. and Porter, M.A.: Detection of core–periphery structure in networks using spectral methods and geodesic paths. European Journal of Applied Mathematics, 27(6), pp.846-887 (2016).
9. Rombach, M.P., Porter, M.A., Fowler, J.H. and Mucha, P.J.: Core-periphery structure in networks. SIAM Journal on Applied mathematics, 74(1), pp.167-190 (2014).
10. Yu, X., Hu, D., Zhang, L. Huang, Y., Wu, Z., Liu, T., Wang, Li., Lin, W., Zhu, D., and Li, G.: Longitudinal infant functional connectivity prediction via conditional intensive triplet network. In MICCAI, pp.255-264 (2022).
11. Nie, J., Guo, L., Li, K., Wang, Y., Chen, G., Li, L., Chen, H., Deng, F., Jiang, X., Zhang, T. and Huang, L.: Axonal fiber terminations concentrate on gyri. Cerebral cortex, 22(12), pp.165-178 (2012).
12. Yu, X., Zhang, L., Zhu, D., and Liu, T.: Robust Core-Periphery Constrained Transformer for Domain Adaptation. arXiv preprint arXiv:2308.13515 (2023).
13. Yu, X., Zhang, L., Dai, H., Lyu, Y., Zhao, L., Wu, Z., Liu, D., Liu, T. and Zhu, D.: Core-periphery principle guided redesign of self-attention in transformers. arXiv preprint arXiv:2303.15569 (2023).
14. Dosovitskiy, A., Beyer, L., Kolesnikov, A., Weissenborn, D., Zhai, X., Unterthiner, T., Dehghani, M., Minderer, M., Heigold, G., Gelly, S. and Uszkoreit, J.: An image is worth 16x16 words: Transformers for image recognition at scale. arXiv preprint arXiv:2010.11929 (2020).

15. Yu, X., Zhang, L., Zhao, L., Lyu Y., Liu, T., and Zhu, D.: Disentangling spatial-temporal functional brain networks via twin-transformers. arXiv preprint arXiv:2204.09225, (2022).
16. Zhang, W., Lv, J., Li, X., Zhu, D., Jiang, X., Zhang, S., Zhao, Y., Guo, L., Ye, J., Hu, D. and Liu, T.: Experimental comparisons of sparse dictionary learning and independent component analysis for brain network inference from fMRI data. IEEE transactions on biomedical engineering, 66(1), pp.289-299 (2018).
17. Glasser, M.F., Smith, S.M., Marcus, D.S., Andersson, J.L., Auerbach, E.J., Behrens, T.E., Coalson, T.S., Harms, M.P., Jenkinson, M., Moeller, S. and Robinson, E.C.: The human connectome project's neuroimaging approach. Nature neuroscience, 19(9), pp.1175-1187 (2016).
18. Hopfinger, J.B., Büchel, C., Holmes, A.P. and Friston, K.J.: A study of analysis parameters that influence the sensitivity of event-related fMRI analyses. Neuroimage, 11(4), pp.326-333 (2000).
19. Li, G., Liu, T., Ni, D., Lin, W., Gilmore, J.H. and Shen, D.: Spatiotemporal patterns of cortical fiber density in developing infants, and their relationship with cortical thickness. Human brain mapping, 36(12), pp.5183-5195 (2015).
20. Zhang, L., Yu, X., Lyu, Y., Liu, T., and Zhu, D.: Representative Functional Connectivity Learning for Multiple Clinical groups in Alzheimer's Disease. IEEE 20th International Symposium on Biomedical Imaging, pp.1-5 (2023).
21. Yu, X., Zhang, L., Lyu, Y., Liu, T., and Zhu, D.: Supervised Deep Tree in Alzheimer's Disease. IEEE 20th International Symposium on Biomedical Imaging, pp.1-5 (2023).
22. Lyu, Y., Yu, X., Zhu, D., and Zhang, L.: Classification of alzheimer's disease via vision transformer. In Proceedings of the 15th international conference on PErvasive technologies related to assistive environments, pp.463-468 (2022).
23. Lyu, Y., Yu, X., Zhang, L., and Zhu, D.: Classification of mild cognitive impairment by fusing neuroimaging and gene expression data. In Proceedings of the 14th international conference on PErvasive technologies related to assistive environments, pp.26-32 (2021).
24. Yu, X., Scheel, N., Zhang, L., Zhu, D.C. Zhang, R. and Zhu, D.: Free water in T2 FLAIR white matter hyperintensity lesions. Alzheimer's & Dementia, 17, pp.e057398 (2021).
25. Zhang, L., Wang, L., Gao, J., Risacher, S.L., Yan, J., Li, G., Liu, T., Zhu, D. and Alzheimer's Disease Neuroimaging Initiative, 2021. Deep fusion of brain structure-function in mild cognitive impairment. Medical image analysis, 72, p.102082.
26. Zhang, L., Wang, L. and Zhu, D., 2020, April. Jointly analyzing Alzheimer's disease related structure-function using deep cross-model attention network. In 2020 IEEE 17th International Symposium on Biomedical Imaging (ISBI) (pp. 563-567). IEEE.
27. Zhang, L., Zaman, A., Wang, L., Yan, J. and Zhu, D., 2019. A cascaded multi-modality analysis in mild cognitive impairment. In Machine Learning in Medical Imaging: 10th International Workshop, MLMI 2019, Held in Conjunction with MICCAI 2019, Proceedings 10 (pp. 557-565).
28. Zhang, L., Wang, L., Liu, T. and Zhu, D., 2024. Disease2Vec: Encoding Alzheimer's progression via disease embedding tree. Pharmacological Research, 199, p.107038.
29. Zhang, L., Na, S., Liu, T., Zhu, D. and Huang, J., 2023, October. Multimodal deep fusion in hyperbolic space for mild cognitive impairment study. In MICCAI (pp. 674-684). Cham: Springer Nature Switzerland.
30. Zhang, L., Zhao, L., Liu, D., Wu, Z., Wang, X., Liu, T. and Zhu, D., 2023. Cortex2vector: anatomical embedding of cortical folding patterns. Cerebral Cortex, 33(10), pp.5851-5862.